



HAL
open science

Identification of fetal liver stroma in spectral cytometry using the parameter autofluorescence†

Marcia Mesquita Peixoto, Francisca Soares-da-silva, Sandrine Schmutz, Marie-pierre Mailhe, Sophie Novault, Ana Cumano, Cedric Ait-mansour

► To cite this version:

Marcia Mesquita Peixoto, Francisca Soares-da-silva, Sandrine Schmutz, Marie-pierre Mailhe, Sophie Novault, et al.. Identification of fetal liver stroma in spectral cytometry using the parameter autofluorescence†. Cytometry Part A, 2022, 10.1002/cyto.a.24567 . pasteur-03663861

HAL Id: pasteur-03663861

<https://pasteur.hal.science/pasteur-03663861>

Submitted on 10 May 2022

HAL is a multi-disciplinary open access archive for the deposit and dissemination of scientific research documents, whether they are published or not. The documents may come from teaching and research institutions in France or abroad, or from public or private research centers.

L'archive ouverte pluridisciplinaire **HAL**, est destinée au dépôt et à la diffusion de documents scientifiques de niveau recherche, publiés ou non, émanant des établissements d'enseignement et de recherche français ou étrangers, des laboratoires publics ou privés.

What are you missing in your research?

Highly sensitive, flexible flow cytometry

Amnis[®] CellStream[®] Flow Cytometry System



For Research Use Only. Not for use in diagnostic procedures.

Luminex[®]
complexity simplified.

Novault Sophie (Orcid ID: 0000-0001-5708-3597)

Cumano Ana (Orcid ID: 0000-0002-4578-959X)

Identification of fetal liver stroma in spectral cytometry using the parameter autofluorescence⁹

Marcia Mesquita Peixoto^{1,2,3,4,5,6+}, Francisca Soares-da-Silva^{1,2,3+}, Sandrine Schmutz⁷, Marie-Pierre Mailhe^{1,2,3}, Sophie Novault^{7#}, Ana Cumano^{1,2,3#*} & Cedric Ait-Mansour^{8#}

¹Unit Lymphocytes and Immunity, Immunology Department,

²INSERM U1223, Paris, France

³Université de Paris, Sorbonne Paris Cité, Paris, France

⁴Instituto de Investigação e Inovação em Saúde, Universidade do Porto, Porto, Portugal

⁵Instituto Nacional de Engenharia Biomédica, Universidade do Porto, Porto, Portugal

⁶Instituto de Ciências Biomédicas Abel Salazar, Universidade do Porto, Porto, Portugal

⁷Flow cytometry core facility, CRT2, Institut Pasteur, Paris, France

⁸Sony Europe B.V

⁹This work was supported by grants from Institut Pasteur, INSERM, ANR and FCT/MCTES.

* Corresponding author

Ana Cumano, Immunology Department

Institut Pasteur 25 Rue du Dr. Roux 75724 Paris, CEDEX 15, France.

Tel +33145688255

Fax +33145688921

Email : ana.cumano@pasteur.fr

ORCID: 0000-0002-4578-959X

This article has been accepted for publication and undergone full peer review but has not been through the copyediting, typesetting, pagination and proofreading process which may lead to differences between this version and the [Version of Record](#). Please cite this article as doi: [10.1002/cyto.a.24567](https://doi.org/10.1002/cyto.a.24567)

This article is protected by copyright. All rights reserved.

+ Equal contribution

Co-senior authors

Key words: Spectral flow cytometry; autofluorescence; fetal liver; hepatoblast-like cells/hepatocytes

Autofluorescence patterns in fetal liver

Abstract

The fetal liver is the main hematopoietic organ during embryonic development. The fetal liver is also the unique anatomical site where hematopoietic stem cells expand before colonizing the bone marrow, where they ensure life-long blood cell production and become mostly resting. The identification of the different cell types that comprise the hematopoietic stroma in the fetal liver is essential to understand the signals required for the expansion and differentiation of the hematopoietic stem cells. We used a panel of monoclonal antibodies to identify fetal liver stromal cells in a 5-laser equipped spectral flow cytometry analyzer. The “Autofluorescence Finder” of SONY ID7000 software identified two distinct autofluorescence emission spectra. Using autofluorescence as a fluorescence parameter we could assign the two autofluorescent signals to three distinct cell types and identified surface markers that characterize these populations. We found that one autofluorescent population corresponds to hepatoblast-like cells and cholangiocytes whereas the other expresses mesenchymal transcripts and was identified as stellate cells. Importantly, after birth, autofluorescence becomes the unique identifying property of hepatoblast-like cells because mature cholangiocytes are no longer autofluorescent.

These results show that autofluorescence used as a parameter in spectral flow cytometry is a useful tool to identify new cell subsets that are difficult to analyze in conventional flow cytometry.

Introduction

Flow cytometry (FCM) has rapidly evolved over the past few decades (1). The development of more advanced technologies including mass cytometry (2), imaging flow cytometry (3), genomic flow cytometry (4) and spectral flow cytometry (5), has expanded our ability to study immune responses, by characterizing more cellular parameters simultaneously in single cells with higher resolution than ever before. FCM characterizes physical and fluorescent properties of cells in suspension by using fluorochrome-conjugated antibodies to measure proteins expressed by distinct immune cell subpopulations (6).

Spectral flow cytometry was first proposed by J. Paul Robinson at Purdue University in 2004 (7). The first commercial instrument (Sony SP6800) was launched by Sony Biotechnology in 2012, using prisms along with PMT detectors to collect and amplify light beyond the capability of conventional flow cytometers (8). The Sony SP6800 is equipped with three lasers 405/488/638nm and two pinholes such that two excitation lasers can be used in a given experiment. Using the 405/488nm excitation lasers we assembled a 19-fluorescent probe panel to analyze immune cells in the mouse adult spleen (9, 10). Moreover, analysis of antibody-stained preparations of embryonic, neonatal and adult heart, which is a highly auto-fluorescent tissue, allowed the robust identification of new surface markers of different cardiac populations (11). In addition, intra-epithelial lymphocytes were efficiently analyzed in mouse intestinal epithelium cell preparations because the autofluorescence management allowed eliminating from the analysis the autofluorescent epithelial cells (9). Recently, the Sony ID7000 became available with different laser configurations that can be remodeled. The ID7000 Software analysis is based on the previously described Weighted Least Squares

Method (WLMS) algorithm (8) that allows the easy detection of auto-fluorescence (AF) that can be incorporated in the panel as independent fluorescent parameters.

The fetal liver (FL) is a highly auto-fluorescent tissue where hepatic and hematopoietic cells differentiate alongside and where hepatic and mesenchymal cells play, yet ill-defined, roles in hematopoietic differentiation (12) and in the establishment of the hematopoietic stem cell compartment (13). In addition, although surface markers for different populations have been identified, a global analysis of the FL stroma using epithelial and mesenchymal markers has not been undertaken.

Here we sought to analyze the non-hematopoietic stromal compartment in mouse FL using a 14-fluorochrome antibody panel and distinct AF parameters that were unique in the identification of cell populations. We found two major AF signals at embryonic day (E)18.5 of mouse gestation. One AF signal has different emission spectra in the 355nm laser and in the 405nm laser. It defines stellate cells that accumulate autofluorescent vitamin A in cytoplasmic granules (14). The second AF signal is visible in the 355 nm laser, in the 405 nm and also with a lower intensity and different emission spectra in the 488 and 561nm lasers and marks hepatoblasts/hepatocytes and cholangiocytes. Importantly, AF is an invaluable tool to distinguish cells with the characteristics of E14.5 hepatoblasts, after birth, hereafter designated as hepatoblast-like cells. In addition, defining the true fluorescence associated with each autofluorescent population helped design a sorting strategy to be used in conventional FCM. These results indicate that AF treated as a fluorescence parameter in spectral flow cytometry is essential to the characterization of cell subsets in solid tissues.

Materials and Methods

The experiment was designed to identify populations of stromal cells in the mouse fetal liver at different stages of gestation

Cell suspension

E14.5, E18.5 fetal livers (FL), P3 and P9 livers were dissected under a binocular magnifying lens. Cells were recovered in Hanks' balanced-salt solution (HBSS) supplemented with 1% fetal calf serum (FCS) (Gibco) or RPMI medium (Gibco) supplemented with 10% FCS (P3 and P9) and treated with 0.05 mg/ml Liberase TH (Roche) and 0.2 mg/ml DNase (Sigma) for 6-8 minutes at 37°C. Cells were resuspended by gentle pipetting. Before staining, cell suspensions were filtered with a 100 µm cell strainer (BD). All experiments using E14.5 and E18.5 embryos were done by pooling FL cells from the same litter in each experiment, in three or more biological replicates. In an independent experiment, fetal liver cells were analyzed after mechanical dissociation (in two biological replicates; *data not shown*).

Flow sample and specimen description

All antibodies were titrated to give the highest signal-to-noise ratio. The antibody panel has been optimized in a conventional flow cytometer (LSR Fortessa with 5 lasers (BD Biosciences) and then used in the ID7000 (Sony) to study the autofluorescence. Liver cells were depleted of Ter119⁺ CD45⁺ CD71⁺ CD117⁺ cells by magnetic cell separation using LS MACS Columns (Miltenyi Biotec). Cell suspensions were stained in two steps. First, cell suspensions of fetal liver were incubated with the biotinylated antibodies for 15-20 min at 4°C. Cells were washed to eliminate excess of antibody, incubated for 15 minutes with anti-biotin beads (Miltenyi Biotec) and applied to a LS MACS Column (Miltenyi Biotec). 5% of the cells were not passed

through the MACS column and were used as depletion control. 5% of the eluted cells were used as unstained control and the remaining were incubated for 20-30 min at 4°C in the dark with directly labelled antibodies (and streptavidin (SAV) listed in Table 1/Supplemental Table 1. PI was added to depleted stained and to the depletion control samples.

Instrument details

Stained cells were analyzed in the Sony ID7000 spectral cytometer. The LE-ID7000E used in this study has 5 lasers 355/405/488/561/637nm (Supplemental Figure 1), PMT gains/voltages can be independently adjusted for each laser and there are 7 pinholes allowing for additional lasers to be installed. The schematic optical configuration is shown in Supplemental Figure 1, framed by a black box. The detection capacity of the ID7000 spans from 360 nm to 820 nm in the 5-laser configuration. The signals are captured with 32-, 26- and 19-channel PMT arrays and individual PMT, as shown.

Before the analysis, the Sony ID7000 was calibrated using the align-check and the performance 8-peak beads, following the guidelines of the instrument provider. A minimum of 100000 events were acquired for cell-stained samples and a minimum of 20000 events for unstained samples. In every experiment single-stained samples in Ultracomp eBeads (Thermo Fisher), for each individual fluorochrome, were provided and a minimum of 2000 events were collected. Total FL cells stained with propidium iodide (PI) were used as the control for dead cell exclusion. Unstained cells after depletion were always included. Stained cells with the full panel, before depletion of hematopoietic cells, were analyzed as a control for lineage staining.

Data analysis details

Autofluorescence analysis

The unstained samples, after depletion of hematopoietic cells, were analyzed using the autofluorescence finder function as shown in Figure 2. This is a non-automatic visualization tool where scanning across the emission wavelengths on each laser detects the best display of autofluorescence. The scanning is done by moving the cursor (bar under top plots in Figure 2) and the signal in the different combined detectors can be adjusted to find the best separation between the different autofluorescence signals. The autofluorescence signals are then manually gated and checked for their emission spectra (see Figure 2, lower panels). Distinct autofluorescence signals will separate in one of the laser combinations and will have distinct emission spectra. Once identified the autofluorescence signals are incorporated in the unmixing matrix.

Acquired full spectrum are analyzed with algorithms based on the WLSM as described previously (8). The accuracy of the unmixing is ensured by the analysis of the single stained samples. Further manual adjustments (usually not required) can be done. Acquisitions were done with similar settings of the laser PMT.

Cells were sorted with a BD FACSAria III (BD Biosciences) according to the guidelines for the use of FCM and cell sorting (6). The FACSAria III was calibrated with CST beads following the manufacturer's protocols. Data were analyzed with the ID7000 (Sony, Inc) or FlowJo (v.10.7.3, BD Biosciences) software.

Gene expression by RT-PCR

Cells were sorted directly into lysis buffer and mRNA was extracted with a RNeasy Micro Kit (Qiagen). After extraction mRNA was reverse-transcribed into cDNA with PrimeScript RT

Accepted Article

Reagent Kit (Takara Bio), followed by quantitative PCR with Power SYBR Green PCR Master Mix (Applied Biosystems). Primers used were as follows: Actb FW: GCTTCTTTGCAGCTCCTTCGT; Actb RV: ATCGTCATCCATGGCGAACT; Afp FW: CTTCCCTCATCCTCCTGCTAC; Afp RV: ACAAACTGGGTAAAGGTGATGG; Alb FW: TGCTTTTTCCAGGGGTGTGTT; Alb RV: TTA CTTCTGCACTAATTTGGCA; Des FW: GTGGATGCAGCCACTCTAGC; Des RV: GTGGATGCAGCCACTCTAGC; Onecut1 FW: GCCCTGGAGCAAACCTCAAGT; Onecut1 RV: TTGGACGGACGCTTATTTTCC; Pdgfrb FW: TTCCAGGAGTGATACCAGCTT; Pdgfrb RV: AGGGGGCGTGATGACTAGG; Sox9 FW: CTCCTCCACGAAGGGTCTCT; Sox 9 RV: AGGAAGCTGGCAGACCAGTA. qPCR reactions were performed on a Quantstudio3 thermocycler (Applied Biosystems), gene expression was normalized to that of β -actin and relative expression was calculated using the $2^{-\Delta Ct}$ method.

Statistical analysis

All results are shown as mean \pm standard deviation (SD). Statistical significance was determined using one-way ANOVA followed by Tukey's multiple comparison test where a P value <0.05 was considered significant and a P value >0.05 was considered not significant.

Results

A strategy to characterize non-hematopoietic cell populations in fetal liver

To characterize non-hematopoietic (hereafter referred to as stromal) populations in the FL we assembled a panel of 14 fluorescent dyes (Table 1) that included propidium iodide (PI- dead cell exclusion) and 13 fluorescence conjugated antibodies that mark cells belonging to the hepatic, endothelial and mesenchymal lineages (liver fibroblasts, also called stellate cells - see Table 1). The analysis was done in FL cell suspensions depleted of hematopoietic cells in a dump channel that includes the erythroid marker TER119, the pan-hematopoietic marker CD45, and CD71 and CD117 that together mark embryonic erythroid progenitors (15). Cells were depleted of hematopoietic cells, that represent more than 80% of total FL cells, by magnetic sorting. We analyzed liver cells isolated from embryonic days (E) 14.5 and E18.5 (one day prior to birth), and from days 3 and 9 post-birth (P3 and P9). Figure 1A shows the spectra of emission of E18.5 cells after the elimination of hematopoietic and dead cells. Figure 1B shows the gating strategy used to identify known cell subsets with CD31 and CD146 defining endothelial cells, and, in non-endothelial cells, CD140a (PDGFRa), Gp38 (podoplanin), and CD166 (ALCAM) define stellate cells as CD140a⁺Gp38⁻CD116⁺ (13). In the Gp38⁻CD140a⁻ subset, CD326 and CD324 (E-Cadherin) define cholangiocytes (CD324⁺CD326⁺)(16) and hepatic cells (CD324^{high/low} CD326⁻) (17) . This analysis shows that at E18.5 all major FL populations are detected, and hepatocytes are difficult to discriminate from the decreasing numbers of hepatoblasts that are undergoing differentiation.

Two different autofluorescence patterns identified by the autofluorescence finder

AF is a property of many tissues defined as signal emission by cells excited at particular wavelengths, in the absence of specific fluorescence. AF can mask or distort true fluorescence and is usually subtracted to facilitate the fluorescence detection. The ID7000 spectral cytometer is equipped with an analytical software that provides a tool to identify independent AF signals called AF finder (Figure 2, see Materials and Methods). In unstained cells this tool allowed the detection of two AF signals (Figure 2A). AF-1 is detected with the 355, and 405nm lasers with decreasing intensity and more importantly different emission spectra, and virtually undetected with the remaining lasers. AF-2 is detected with the 355 and 405 nm lasers, with distinct spectra of emission, is also detected with the 488 and 561 nm lasers and virtually undetected with the 637 nm laser. The differences in the spectra of emission found in most laser channels suggested that these two AF signals correspond to two independent cell types. Efficient single cell suspension that minimizes cell death requires an enzymatic digestion of the fetal liver. To test whether the two autofluorescence signals were impacted by the enzymatic digestion we analyzed E14.5 fetal liver after mechanic dissociation. The autofluorescent signals were detected after mechanic dissociation (*data not shown*) indicating that they are an intrinsic property of the two subsets. The frequencies and numbers of cells exhibiting AF-1 and AF-2 were, however, strongly reduced consistent with our previous observation that mechanical dissociation is not suited for FL viable cell recovery. After unmixing, we used AF-1 and AF-2 as independent parameters to define two different populations and proceeded to identify their identity (Figure 3 A-D). Figure 3 shows two independent gating strategies, one that analyzes cells within AF-1 (Figure 3B) compared to the conventional strategy previously shown in Figure 1 (Figure 3A). AF-1 cells correspond to a majority of CD31⁻ (85%), CD140a⁺ (85%) cells and CD116⁺ (95%) cells (Figure 3B) that define, with a high degree of enrichment, stellate cells.

Accepted Article

CD324⁺ hepatocytes and CD324⁺CD326⁺ cholangiocytes (bile duct cells) are known to derive during embryonic development from bipotent progenitors called hepatoblasts (18). AF-2 gated cells (Figure 3C) comprise a majority (83%) of CD31⁻ non-endothelial cells, 94% of CD140a⁻ gp38⁻ and >90% of CD324^{high}. We designated this population hepatoblasts-like cells because they closely resemble cells with similar phenotype and autofluorescent properties in E14.4 FL, before cholangiocyte differentiation (Supplemental Figure 2), known to be bipotent progenitors (16). Within AF-2 in E18.5 FL we also found CD324⁺ CD326⁺ cholangiocytes (19). Interestingly, the analysis done in AF-2 did not detect the subset that expresses low levels of CD324 that we classify as hepatocytes (17) (Figure 3C). AF-2 is, therefore, an important parameter to distinguish hepatoblasts-like cells from hepatocytes, at this stage of development. When auto-fluorescent cells were gated out, stellate cells are virtually absent from the plots (Figure 3D) whereas a subset of hepatoblasts-like cells and cholangiocytes are still detected (30% and 50%, respectively) indicating that AF-2 distinguishes two different cell subsets (AF-2⁺ and AF-2⁻ cells) in each of these populations. The cells designated as non-AF correspond to cells with low AF-1 and AF-2 and comprise all other cell populations in the FL that exhibit background levels of AF.

Properties and identity of fetal liver stromal cells

To further characterize the AF of FL cells and determine whether this is a cell-intrinsic property or if it is lost upon manipulation we sorted hepatic cells, hepatoblast-like cells and stellate cells from E18.5 FL using a simplified panel in a conventional flow cytometer (Figure 4A, pre-sort). All populations before and after cell sorting were analyzed in spectral FCM (Figure 4B, sorted populations). Stellate cells (lower plots) show persistent levels of AF whereas hepatocytes (upper plots) remained negative for this parameter. As previously observed,

hepatoblast-like cells sorted as CD324^{high} cells yield a mixed population of AF-2⁺ and AF-2⁻ cell (middle plots). These results indicated that AF in fetal liver populations is a cell-specific property.

In order to unambiguously ascertain the lineage affiliation of these three cell subsets we subjected the cells sorted to quantitative RT-PCR. We show that cells classified as cholangiocytes by flow cytometry express the cholangiocyte markers *Sox9* and *Onecut 1* (*Hnf6*) (16), the hepatoblast-like cells express *Onecut 1* (18), *Alb* and *Afp* whereas stellate cells express *Desmin* and *Pdgfrb* (Figure 4C) (20). This transcriptional profile is specific for the three subsets thus confirming the lineage affiliation inferred by the surface marker expression.

Autofluorescence defines hepatoblast-like cells after birth

Hepatoblast-like cells decrease in numbers as development progresses, so we used AF-2 to detect these cells, after birth. However, hepatocytes that are the dominant liver population after birth are fragile epithelial cells, highly sensitive to manipulation *ex vivo* and to the disruption of the tight junctions, required for single-cell suspensions. Consequently, we detected decreasing numbers of hepatocytes with age. At P3 and P9 the levels of AF were very similar in spectrum and intensity to those seen at E18.5. At P3 and P9 AF-2 represents a majority of hepatoblast-like cells with high expression of CD324, and by high AF-2 (Figure 5A). Interestingly, at these stages, most cholangiocytes lost expression of AF-2. This result is reinforced at P9 (Figure 5B) where gating in AF-2 yields 93% of hepatoblast-like cells. These results further indicate that AF-2 is essential for the identification of hepatoblast-like cells, after birth.

Discussion

In this report we used a spectral flow cytometer equipped with 5 lasers to analyze a highly autofluorescent tissue, the FL, in single-cell suspensions. The software analysis of the Sony ID7000 is equipped with an analytical tool for easy detection of different autofluorescent signals. The unmixing algorithm subtracts the AF to find true fluorescent signals but importantly, by using the AF signals as independent parameters, it increased the panel of 14-fluorescent dyes into a 16-fluorescence panel.

The “Autofluorescence finder” tool identified independent AF signals that differed in shape and intensity in the different laser detectors. Gating on AF-1 we identified a dominant population with the phenotype that defines stellate cells, the fibroblasts specific to the liver. This population has previously been reported to be endowed with AF in a limited analysis using conventional FCM because stellate cells store vitamin A in cytoplasm granules (14). The second AF signal, AF-2, was found in epithelial cells (expressing CD324) that, at E18.5, could be subdivided into two subsets. The first expressed CD326 which is specific, at this stage, of newly differentiated cholangiocytes (19), and the second expressed the highest levels of CD324 while lacking CD326 and was consequently classified as hepatoblasts-like cells because they resemble E14.5 hepatoblasts (16, 17).

Irrespective of the cell preparation method, enzymatic digestion or mechanical dissociation, the two autofluorescent signals were detected, although mechanical dissociation resulted in lower representation of stellate cells and hepatoblast-like cells. We conclude that the two independent AF signals in stromal FL populations were intrinsic properties of the cells which confers reliability to the analysis. The transcriptional profile of the AF populations unambiguously confirmed the lineage affiliation proposed by the surface marker analysis.

The AF-2 parameter allowed the distinction of hepatocytes from hepatoblast-like cells (CD324⁺ CD326⁻ cells), by clearly demarcating the limits between the two cell types. Because hepatoblast-like cells rapidly decrease after birth, as most proliferative activity in the adult liver is driven by hepatocytes, we analyzed liver cells after birth. We found that the two different AF signals persisted at these later time points with AF-2 marking a majority of hepatoblast-like cells. Interestingly, most cholangiocytes lost AF-2 at P3 and virtually all were AF2⁻ at P9. AF-2 is therefore the only property specific for hepatoblast-like cells, after birth. Although hepatocytes are the most numerous cells in the adult liver, they comprised less than 20% of the cell suspension analyzed here. This observation is consistent with the well-documented fragility of hepatocytes. The protocols currently recommended to isolate viable hepatocytes include enzymatic digestion similar to the procedure used in this study (21). Alternatively, a perfusion with an enzymatic solution is followed by a purification in a Percoll gradient (22). In any of these methods, 5-20 x10⁶ hepatocytes (21) (1-6%) can be obtained out of the 3x10⁸ hepatocytes in a mouse liver (23) indicating that no efficient procedure is currently available to isolate hepatocytes.

Our study presents several innovations: 1. The ID7000 software analysis provides an easy tool to detect independent AF signals; 2. The unmixing algorithm subtracts the AF signals to allow accurate true fluorescence detection, a feature already present in the SP6800; 3. Importantly, the analytical tool treats the AF signals as fluorescence and increases, therefore, the panel of analyzed parameters. We provide evidence that these advances will be invaluable to the characterization of single-cell suspensions obtained from autofluorescent tissues, difficult to analyze in conventional FCM.

Acknowledgements

We thank all members of the flow cytometry core facility, the members of the Institut Pasteur laboratory, Antonio Bandeira, Paulo Vieira, Rachel Golub and Pablo Pereira. This work was financed by the Institut Pasteur, INSERM, ANR (grant Twothyme, grant DELSTAR and grant EPI-DEV), REVIVE Future Investment Program and Pasteur-Weizmann Foundation through grants to A.C. This work was financed by Portuguese funds through FCT/MCTES in the framework of the project PTDC/MED-OUT/32656/2017 (POCI-01-0145-FEDER-032656). F.S.S is funded by the REVIVE Future investments post-doctoral grant (Investissement d'Avenir; ANR-10-LABX-73). MP is funded by FCT grant SFRH/BD/143605/2019.

Data availability statement

A version of this manuscript is available in BioRxiv

bioRxiv 2021.09.29.462345; doi: <https://doi.org/10.1101/2021.09.29.462345>

Flow cytometry data has been deposited in Flow Repository under the name "Fetal liver autofluorescence".

Author contribution

Marcia Peixoto did conceptualization, data curation, formal analysis, contributed to investigation, methodology and manuscript writing

Francisca Soares-da-Silva did conceptualization, data curation, formal analysis, contributed to investigation, methodology and manuscript writing.

Sandrine Schmutz did data curation, formal analysis, contributed to methodology.

Marie-Pierre Mailhe did data curation and formal analysis.

Sophie Novault did conceptualization, data curation, formal analysis, contributed to investigation, methodology, supervision and manuscript writing

Ana Cumano did conceptualization, data curation, funding acquisition, project administration, supervision and manuscript writing

Cedric Ait-Mansour did conceptualization, data curation, formal analysis, contributed to investigation, methodology, project administration, supervision and validation.

Disclosures: Cedric Ait-Mansour is working for the company Sony Europe B.v as a global senior manager market development-new products. All other authors declare no competing interests.

References

1. Robinson JP. Spectral flow cytometry-Quo vadimus. *Cytometry A* 2019;95:823.
2. Spitzer MH, Nolan GP. Mass Cytometry: Single Cells, Many Features. *Cell* 2016;165:780.
3. Basiji DA. Principles of Amnis Imaging Flow Cytometry. *Methods Mol Biol* 2016;1389:13.
4. Stoeckius M, Hafemeister C, Stephenson W et al. Simultaneous epitope and transcriptome measurement in single cells. *Nat Methods* 2017;14:865.
5. Nolan JP, Condello D. Spectral flow cytometry. *Curr Protoc Cytom* 2013;Chapter 1:Unit1.27.
6. Cossarizza A, Chang HD, Radbruch A et al. Guidelines for the use of flow cytometry and cell sorting in immunological studies (second edition). *Eur J Immunol* 2019;49:1457.
7. Grégori G, Patsekina V, Rajwa B et al. Hyperspectral cytometry at the single-cell level using a 32-channel photodetector. *Cytometry A* 2012;81:35.
8. Futamura K, Sekino M, Hata A et al. Novel full-spectral flow cytometry with multiple spectrally-adjacent fluorescent proteins and fluorochromes and visualization of in vivo cellular movement. *Cytometry A* 2015;87:830.
9. Schmutz S, Valente M, Cumano A et al. Spectral Cytometry Has Unique Properties Allowing Multicolor Analysis of Cell Suspensions Isolated from Solid Tissues. *PLoS One* 2016;11:e0159961.
10. Schmutz S, Valente M, Cumano A et al. Analysis of Cell Suspensions Isolated from Solid Tissues by Spectral Flow Cytometry. *J Vis Exp* 2017

- Accepted Article
11. Valente M, Resende TP, Nascimento DS et al. Mouse HSA+ immature cardiomyocytes persist in the adult heart and expand after ischemic injury. *PLoS Biol* 2019;17:e3000335.
 12. Pinho S, Frenette PS. Haematopoietic stem cell activity and interactions with the niche. *Nat Rev Mol Cell Biol* 2019;20:303.
 13. Soares-da-Silva F, Peixoto M, Cumano A et al. Crosstalk Between the Hepatic and Hematopoietic Systems During Embryonic Development. *Front Cell Dev Biol* 2020;8:612.
 14. Kubota H, Yao HL, Reid LM. Identification and characterization of vitamin A-storing cells in fetal liver: implications for functional importance of hepatic stellate cells in liver development and hematopoiesis. *Stem Cells* 2007;25:2339.
 15. Soares-da-Silva F, Freyer L, Elsaid R et al. Yolk sac, but not hematopoietic stem cell-derived progenitors, sustain erythropoiesis throughout murine embryonic life. *J Exp Med* 2021;218
 16. Yang L, Wang WH, Qiu WL et al. A single-cell transcriptomic analysis reveals precise pathways and regulatory mechanisms underlying hepatoblast differentiation. *Hepatology* 2017;66:1387.
 17. Nierhoff D, Levoci L, Schulte S et al. New cell surface markers for murine fetal hepatic stem cells identified through high density complementary DNA microarrays. *Hepatology* 2007;46:535.
 18. Si-Tayeb K, Lemaigre FP, Duncan SA. Organogenesis and development of the liver. *Dev Cell* 2010;18:175.
 19. Tanaka M, Okabe M, Suzuki K et al. Mouse hepatoblasts at distinct developmental stages are characterized by expression of EpCAM and DLK1: drastic change of EpCAM expression during liver development. *Mech Dev* 2009;126:665.

20. Tan KS, Kulkeaw K, Nakanishi Y et al. Expression of cytokine and extracellular matrix mRNAs in fetal hepatic stellate cells. *Genes Cells* 2017;22:836.
21. Jung Y, Zhao M, Svensson KJ. Isolation, culture, and functional analysis of hepatocytes from mice with fatty liver disease. *STAR Protoc* 2020;1:100222.
22. Fry JR, Jones CA, Wiebkin P et al. The enzymic isolation of adult rat hepatocytes in a functional and viable state. *Anal Biochem* 1976;71:341.
23. Falconer DS, Gauld IK, Roberts RC. Cell numbers and cell sizes in organs of mice selected for large and small body size. *Genet Res* 1978;31:287.

Figure Legends

Figure 1. **Gating strategy to identify stellate cells, hepatoblasts-like cells, hepatocytes and cholangiocytes.**

E18.5 mouse fetal liver cell suspensions were stained with biotin labelled antibodies recognizing CD45, TER119, CD71, CD117. Negative cells were magnetically sorted and labelled with the antibodies in Table 1. A. The spectra of emission of fetal liver cells after depletion (marked with streptavidin in a dump channel) and gated out of PI labelled cells. B. After unmixing, cells were manually gated to define endothelial, hepatic and stellate cells. The analysis started with a FSC_A/SSC_A gate, doublet exclusion and PI positive/SAV positive cell exclusion. The gate for SAV exclusion was set by the depletion control sample (not depleted). CD324 was defined as a marker of epithelial cells, cholangiocytes $CD324^{high}CD326^{+}$; hepatocytes $CD324^{low}CD326^{-}$; hepatoblasts-like cells $CD324^{high}CD326^{-}$. Stellate cells are defined by as $PDGFR\alpha^{+}CD166^{+}$.

Figure 2. **Autofluorescence finder.**

The analytical tool autofluorescence applied to unstained cells before unmixing. A. Autofluorescence is defined manually in cells that show fluorescence in the different lasers, as defined in Materials and Methods. B. The spectra of emission of the two defined autofluorescent (AF) signals in the different lasers.

Figure 3. **Two distinct autofluorescent signals: AF-1 defines stellate cells and AF-2 defines a subset of hepatic cells and cholangiocytes.**

After unmixing the two AF signals can be used as two additional fluorescent parameters. **A.** E18.5 FL live CD45⁻TER119⁻CD71⁻CD117⁻ cells were analyzed as in Figure 1B. **B.** Analysis of E18.5 FL live CD45⁻TER119⁻CD71⁻CD117⁻AF1⁺ cells using the same strategy as in Figure 1B. **C.** Analysis of E18.5 FL live CD45⁻TER119⁻CD71⁻CD117⁻AF2⁺ cells using the same strategy as in Figure 1B. **D.** Analysis of E18.5 FL live CD45⁻TER119⁻CD71⁻CD117⁻AF1⁻AF2⁻ cells using the same strategy as in Figure 1B.

Figure 4. **Autofluorescence is a cell intrinsic property.**

A. Fetal liver cells negative for the dump channel and for PI expressing cells were sorted after being stained with a simplified antibody panel including Gp38, CD140a, NG2, CD166, CD324 and CD326. Hepatocytes, hepatoblast-like cells and stellate cells were sorted according to the strategy shown (pre-sort). Sorted cells were reanalyzed in the ID7000 spectral analyzer (sorted populations). Left plots show purity control, right plots show AF of sorted cells.

B. Sorted cholangiocytes, hepatoblast-like cells and stellate cells as in A were subjected quantitative RT-PCR in triplicate samples of two independent experiments for *Sox9*, *Onecut1*, *Alb*, *Afp*, *Desmin* and *Pdgfrb*, and normalized to the expression of β -actin used as house-keeping gene. Data are represented as mean +/- SD. *p<0.05, **p<0.01, ***p<0.001, ****p<0.0001

Figure 5. **AF2 defines hepatoblast-like cells after birth**

Analysis of live CD45⁻TER119⁻CD71⁻CD117⁻ P3 and P9 liver cells in a plot of CD324/CD326 after the conventional gating strategy defined in Figure 1 (left plots) or on the cells gated for AF2 expression (right plots).

Table 1. **List of the antibodies used in this study and their specificity.**

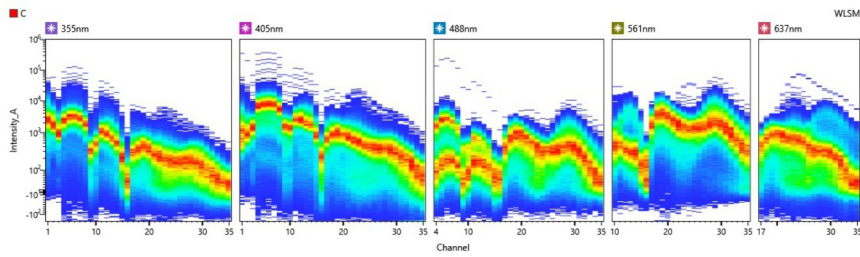
Supplemental Table 1. List of antibodies used in this study indicating the fluorochromes used, the clones of the monoclonal antibodies and the commercial supplier.

Supplemental Figure 1. The optical configuration of the ID 7000 Spectral cytometer. The instrument used in this study has 5 lasers framed by a black box. The 355 nm laser with a 32-channel PMT and two individual PMT, the 405 nm laser with a 32-channel PMT and an individual PMT, a 488 nm laser with a 32-channel PMT, a 561 nm laser with a 26-channel PMT and a 637 nm laser with a 19 channel PMT. Excitation and detection wavelengths spanning from 300 to 900 nm are indicated in the lower bar.

Supplemental Figure 2. Autofluorescence 2 detects hepatoblasts at E14.5. E14.5 fetal liver cells were analyzed as E18.5 in Figure 1 (left panel). AF-2 gated cells detect exclusively CD324⁺ cells (right plot).

Figure 1

A E18.5 FL Live CD45⁻ Ter119⁻ CD71⁻ CD117⁻ cells



B E18.5 FL

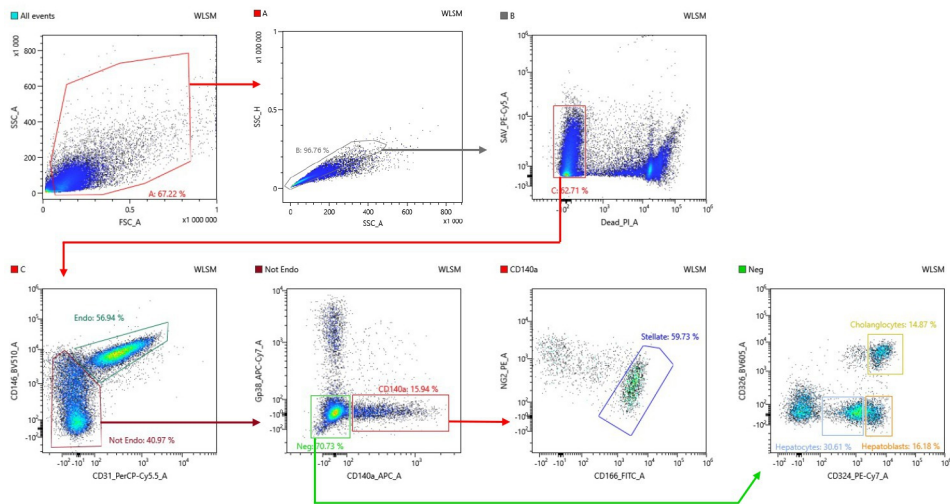


figure-1.eps

Figure 2

A E18.5 FL unstained cells

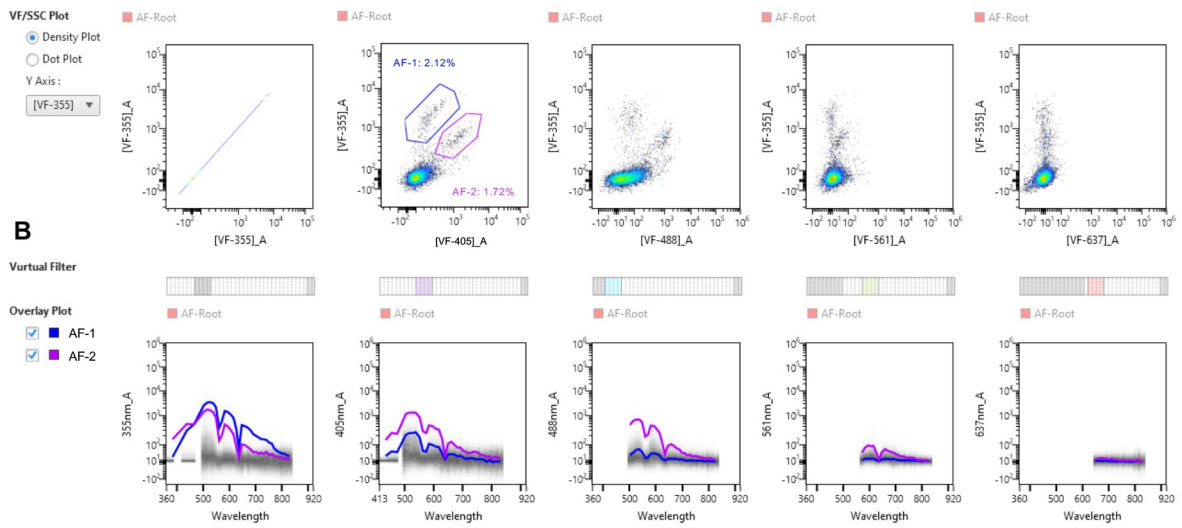


figure-2.eps

Figure 3

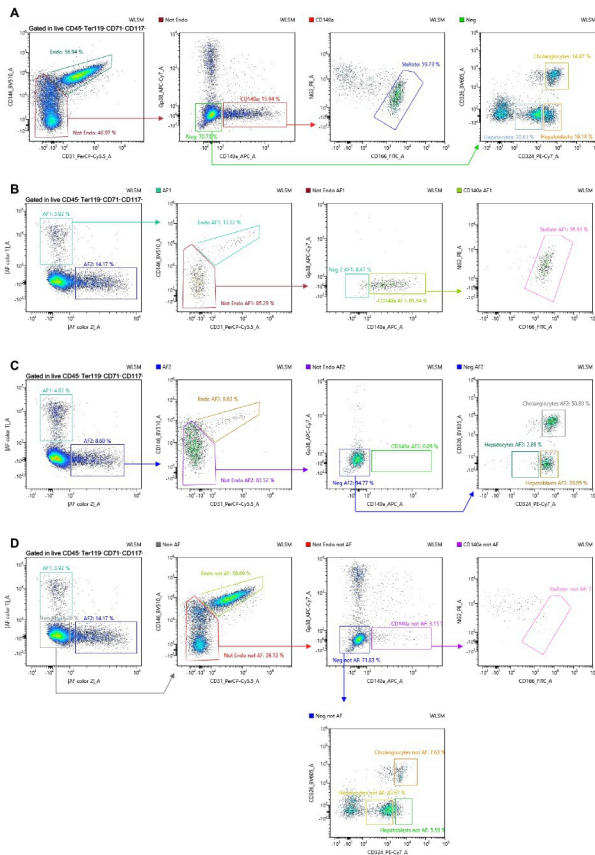


figure-3.eps

Figure 4

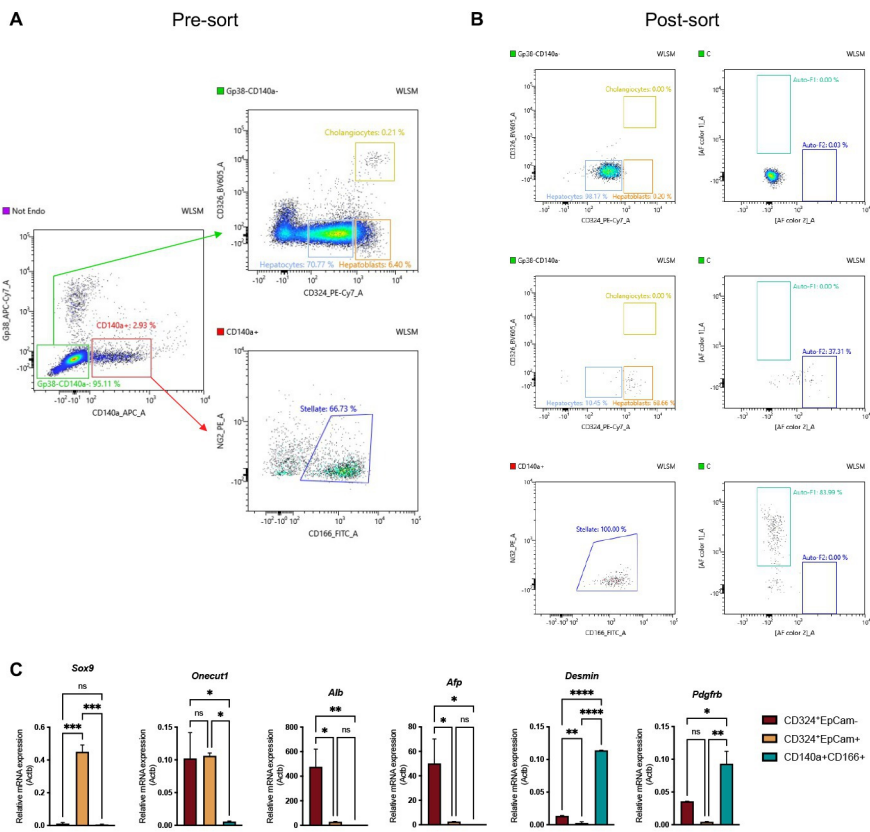


figure-4.eps

Figure 5

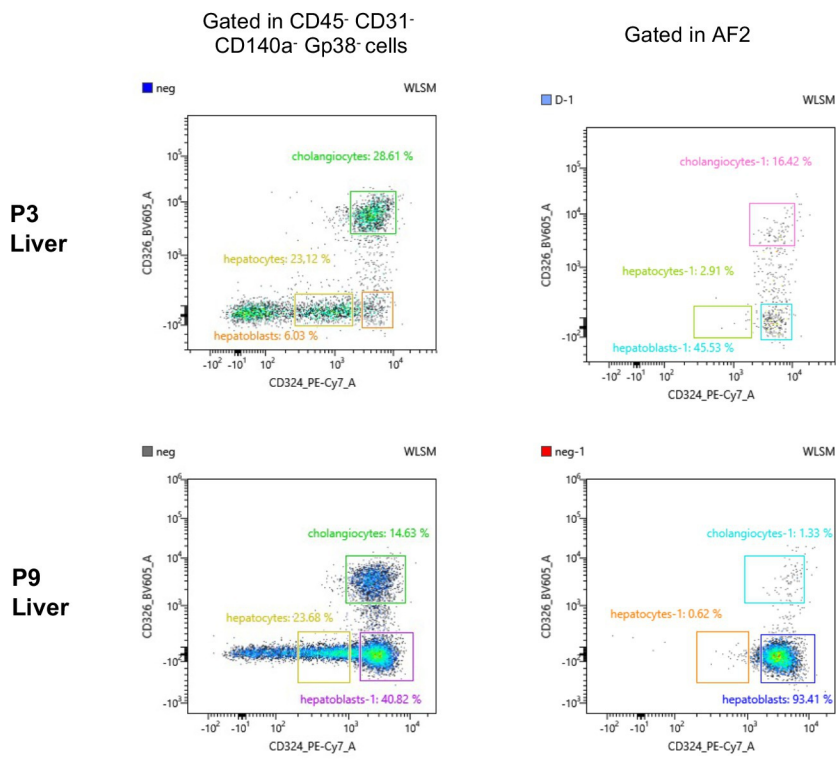


figure-5.eps

Cytometry Part A
Author Checklist: MIFlowCyt-Compliant Items

| Requirement | Please Include Requested Information |
|--|---|
| 1.1. Purpose | The experiment was designed to identify populations of stromal cells in the mouse fetal liver at different stages of gestation. We assembled a 14 fluorescent antibody panel and autofluorescence analyzed in a 5 laser spectral flow cytometer. After conversion with the Sony software we obtained fcs files that are being submitted |
| 1.2. Keywords | [stromal cells] [hematopoiesis] [Fetal liver] |
| 1.3. Experiment variables | |
| 1.4. Organization name and address | Institut Pasteur, Immunology Department 25 Rue du Dr. Roux 75724 Paris CEDEX 15 France |
| 1.5. Primary contact name and email address | Ana Cumano ana.cumano@pasteur.fr |
| 1.6. Date or time period of experiment | <ul style="list-style-type: none"> • Start date: • 2021-02-09 • End date: • 2021-06-30 |
| 1.7. Conclusions | Two distinct autofluorescent patterns can distinguish hepatoblast-like cells and stellate cells in murine fetal liver analyzed at E14.5 and E18.5. |
| 1.8. Quality control measures | All antibodies used in this experiment were previously titrated to give an optimal signal to noise ratio. Before the analysis, the Sony ID7000 was calibrated using the daily QC and the performance 8-peak beads, following the guidelines of the instrument provider. A minimum of 100000 events were acquired for cell-stained samples and a minimum of 20000 events for unstained samples. In every experiment single-stained samples in Ultracomp eBeads (Thermo Fisher), for each individual fluorochrome, were provided and a minimum of 2000 events were collected. Total FL cells stained with propidium iodide (PI) were used as the control for dead cell exclusion. Unstained cells after depletion were always included. Stained cells with the full panel, before depletion of hematopoietic cells, were analyzed as a depletion control. |
| 2.1.1.1. (2.1.2.1., 2.1.3.1.) Sample description | A01 BUV395. Single stained Ultracomp ebeads with anti-mouse CD54 labelled with BUV395 A03 BV711. Single stained Ultracomp ebeads with anti-mouse Sca-1 labelled with BV711 A05 BV605. Single stained Ultracomp ebeads with anti-mouse CD326 labelled with BV605 A07 BV510. Single stained Ultracomp ebeads with anti-mouse CD146 labelled with BV510 A09 BV421. Single stained Ultracomp ebeads with anti-mouse CD51 labelled with BV421 A11 PerCP-Cy5.5. Single stained Ultracomp ebeads with anti-mouse CD31 labelled with PerCP-Cy5.5 |

| | |
|--|---|
| | <p>B02 FITC. Single stained Ultracomp ebeads with anti-mouse CD166 labelled with FITC</p> <p>B04 PE. Single stained Ultracomp ebeads with anti-mouse NG2/AN2 labelled with PE</p> <p>B06 PE-Cy7. Single stained Ultracomp ebeads with anti-mouse CD324 labelled with PE-Cy7</p> <p>B08 PE-Cy5. Single stained Ultracomp ebeads with biotin-stractavidin labelled with PE-Cy5</p> <p>B12 APC-Cy7. Single stained Ultracomp ebeads with anti-mouse gp-38 labelled with APC-Cy7</p> <p>C01 AF700. Single stained Ultracomp ebeads with anti-mouse Thy1.2 labelled with AF700</p> <p>C03 APC. Single stained Ultracomp ebeads with anti-mouse CD140a labelled with APC</p> <p>E02 E14.5 fetal liver cells, depleted of hematopietic cells and stained with the antibody panel in Table 1.</p> <p>E04 E14.5 fetal liver cells, stained with the antibody panel in Table 1.</p> <p>E06 E14.5 fetal liver cells, stained with PI.</p> <p>E08 E14.5 fetal liver cells, depleted of hematopietic cells, unstained.</p> <p>G02 E18.5-1 fetal liver cells, depleted of hematopietic cells and stained with the antibody panel in Table 1.</p> <p>G04 E18.5-2 fetal liver cells, depleted of hematopietic cells and stained with the antibody panel in Table 1.</p> <p>G06 E18.5-2 fetal liver cells, stained with the antibody panel in Table 1.</p> <p>G08 E18.5-2 fetal liver cells, stained with PI</p> <p>G10 E18.5-2 fetal liver cells, depleted of hematopietic cells, unstained</p> |
| 2.1.1.2. Biological sample source description | Mouse fetal liver cells dissociated by enzymatic digestion |
| 2.1.1.3. Biological sample source organism description | Mus Musculus |
| 2.1.2. Environmental sample location | |
| 2.3. Sample treatment description | Enzymatic digestion |
| 2.4. Fluorescenc reagent(s) description | Sup Table 1 |
| 3.1. Instrument manufacture r | Sony iCyt http://www.i-cyt.com/ |
| 3.2. Instrument model | ID 7000 |

| | |
|--|---|
| 3.3. Instrument configuration and settings | Sup Figure 1 and Materials and Methods |
| 4.1. List-mode data files | <p>*We recommend all authors to submit their data files to http://flowrepository.org and to make them available for the peer-review process. If you have done so, please let us know by inserting the following codes (replace the red text):</p> <p>1) The link for peer-review process: Fetal liver autofluorescence (FR-FCM-Z4TE)</p> <p>https://flowrepository.org/id/RvFrk8YZTQYwYro6EaX9fgCAcAhxQyHpNyRQyMxzPuQvh63d1cV8CQ2EqUFNJh4Y</p> |
| 4.2. Compensation description | N/A |
| 4.3. Data transformation details | Data transformation was done with the WLMS as previously described (Futamura et al 2015) |
| 4.4.1. Gate description | |
| 4.4.2. Gate statistics | Done with the Sony analytical software. |
| 4.4.3. Gate boundaries | Manually |

Notes

Feel free to use more space than allocated.

You can embed graphics/figures in this document, if needed.

Please make sure to save the document in Microsoft Word version 2003 or older, before uploading to ScholarOne Manuscripts. When uploading this checklist to ScholarOne Manuscripts, please choose the "Supplementary Material for Review" category.

Please note that if your paper is accepted, the checklist will be published as an Online Supporting Information.

For any questions, please contact the Cytometry Part A editorial office at Cytometrya@wiley.com.

Table 1

| Marker | Conjugation | |
|--------|-------------|--|
| SAV | PE-Cy5 | CD45, TER119, CD71, CD117 (all hematopoietic cells) biotin |
| Dead | PI | - |
| CD324 | PE-Cy7 | (Epithelial-Cadherin) hepatoblasts, hepatocytes and cholangiocytes |
| CD31 | PerCP-Cy5.5 | (Platelet and endothelial cell adhesion molecule) endothelial cells |
| CD166 | FITC | (Activated Leukocyte Cell Adhesion Molecule) hepatoblasts and stellate cells |
| CD140a | APC | (Platelet derived growth factor receptor a) stellate cells and pericytes |
| Gp38 | APC-Cy7 | (Podoplanin) mesenchymal cells, lymphatic endothelial cells |
| NG2 | PE | (Chondroitin sulphate proteoglycan 4) pericytes |
| Sca-1 | BV711 | (Stem Cell antigen 1) endothelial cells |
| CD146 | BV510 | (Melanoma cell adhesion molecule) endothelial cells and mesenchymal cells |
| CD51 | BV421 | (Integrin alpha V) mesenchymal cells |
| CD326 | BV605 | (Epithelial cell adhesion molecule) cholangiocytes (bile duct cells) |
| CD54 | BUV395 | (Intercellular Adhesion Molecule 1) hepatoblasts and endothelial cells |
| Thy1.2 | AF700 | (Cluster of differentiation 90) mesenchymal cells |

table-1.eps